High-Stability Current Control in the 10 A Range

Enrico Rubiola

Abstract— **This paper reports on the design and evaluation of a high-stability current control developed for energizing the C-field magnet of the high-field cesium standard experiment, currently in progress at the Politecnico di Torino. This source must supply about 0.8 kW dc power with a current stability in the 10^{-7} range for more than 1 h.**

I. Introduction

A control circuit is described, capable of stabilizing a 10 A dc current to 10^{-7}. This stability is needed for field uniformity measurements inside the C-field magnet of the high-field cesium frequency standard described in [1]. Since this current control is intended to be used also for normal frequency standard operation, it was decided to avoid chopper amplifiers in order to prevent any possible interference effects of the chopper frequency on other parts of the standard.

The magnet is made of 5400 turns of 3 mm × 1 mm flat copper wire wound on a 70 mm outer diameter, 700 mm long, copper pipe which constitutes the vacuum containment. Two mumetal end caps and an external mumetal flux return tube complete the magnetic circuit. The total weight is about 50 kg. The magnet has a thermal time constant of 2 h when it is energized at its nominal current of 8.6 A and operates at about 70 °C in thermal equilibrium when water cooled. The simplified equivalent circuit of the magnet is a 10.8 Ω resistance in series to a 250 mH inductance; the time constant is $\tau = L/R \simeq 23$ ms, which yields a corner frequency of 7 Hz in the Bode plot of the impedance. Interlayer capacitances generate a parasitic resonance at about 7 kHz. More details about this magnet can be found in [2] and [3].

The field uniformity measurement is performed with a proton nuclear magnetic resonance (NMR) probe which scans the bore axis; this uniformity measurement problem is discussed in detail in [4] and [5]. In order to guarantee internal consistency of an acquisition run, the average field must be adequately stabilized during the whole scan; this must be accomplished by keeping the current constant. Therefore, a stability of about 10^{-7} must be guaranteed for the current in the time range between a few seconds and a couple of hours, which is the maximum measurement time (duration of the scan).

In Section II, the main guidelines are discussed that lead to the proposed design, and the main blocks of the control are described. In Section III the relevant factors that limit the stability and some unusual aspects of precision electronic design are analyzed. In Section IV experimental results are reported and discussed.

Manuscript received July 31, 1995; revised March 4, 1996.

The author is with the Dipartimento di Elettronica, Politecnico di Torino, Torino, Italy.

Publisher Item Identifier S 0018-9456(96)06415-7.

II. Current Control

Current stabilization is achieved by load regulation, as shown in the scheme of Fig. 1. A dc voltage proportional to the current is sensed at the voltage terminals of a reference resistor, amplified and compared with a voltage reference. The output of this is the error signal is integrated in order to drive the power actuator.

The overall design guidelines can be drawn from a preliminary analysis, as follows.

The reference resistor must have a stability of 10^{-7} for a contribution of 10^{-7} to current stability. Under non-airconditioned laboratory conditions, voltage measurements seem to be limited by parasitic thermocouples that can generate emf variations up to about 100 nV; therefore, a specification of 100 nV stability for the electronic circuitry seems to make sense. Consequently, a voltage of 2 V must be available across the reference resistor for a current stability of 10^{-7}. With these design guidelines, the minimum resistance value turns out to be 200 mΩ, given the 10 A current at which the loop is meant to operate.

The 0 dB frequency of the control open-loop gain must be at most 7 Hz. This is because of the magnet impedance, which changes from resistive to inductive as the frequency increases above 7 Hz. Therefore, beyond this frequency, the magnet must be energized by a voltage-stabilized power supply. Otherwise, the conflict between two current generators — the control and the magnet itself, which is a *current stabilizer* at frequencies above 7 Hz — makes the loop hard to stabilize. As a consequence, the ripple specification must be fulfilled by the power supply because the current control can not compensate the ripple. Taking into account the filtering effect of the inductive part of the magnet and the shielding of the copper pipe, a ripple level of less than about 100 μV peak to peak at 50 Hz must be guaranteed.

The dynamic range of the power actuator is not a critical parameter because the control works at a single current value. A range of 10^{-2} is sufficient in order to compensate the variation of the winding resistance due to temperature.

More details are given in the following sections.

A. Reference Resistor

A 0.26 Ω reference resistor was built specifically for this application, keeping in mind that its nominal power dissipation is 20 W. Since this device operates at a single current value, design criteria are slightly different from those adopted for standard resistors. A sketch of the resistor is shown in Fig. 2.

Two manganin wires are wound on an aluminum rod in opposite directions, in order to minimize magnetic coupling to the environment. Windings are thermally coupled to the rod,

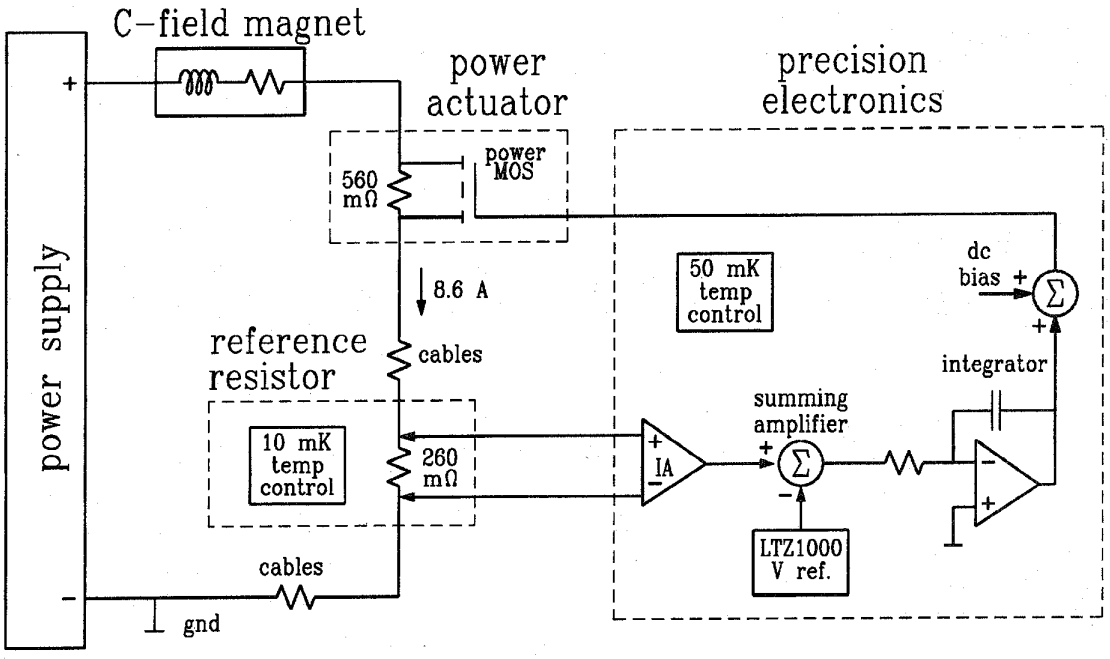

Fig. 1. Block diagram of the proposed control circuit.

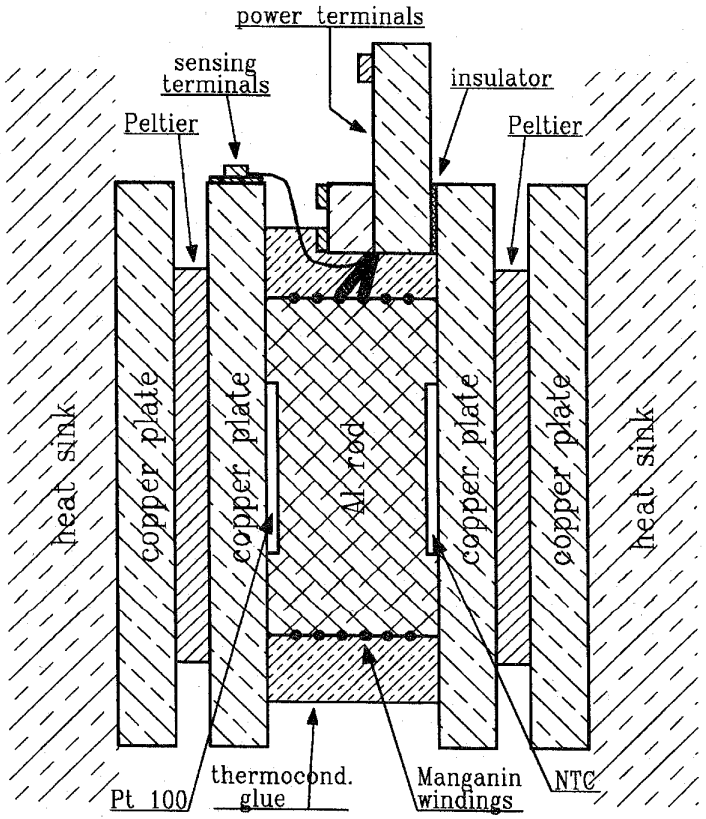

Fig. 2. Reference resistor.

and sealed in thermoconductive glue (thin aluminum powder and epoxy resin).

Manganin alloy (Cu 86 resistance material because of its outstanding electrical characteristics: i) low aging, ii) low

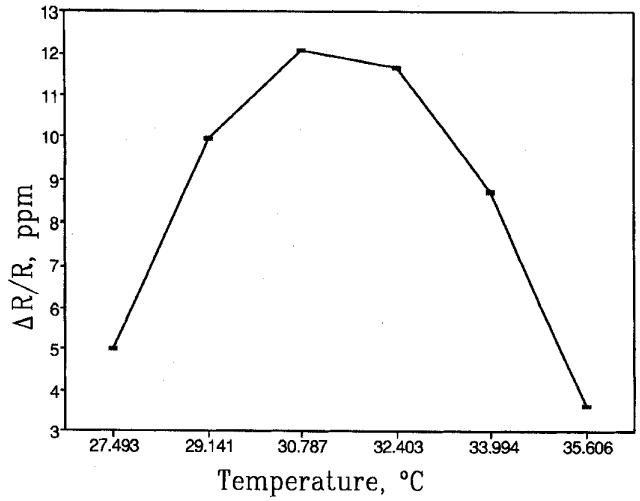

Fig. 3. Measured R versus T characteristics of the reference resistor. The maximum of the fitting parabola occurs at 31.2 °C.

Seebeck coefficient versus copper (about 600 nV/K), and iii) low-temperature coefficient with parabolic shape of the R versus T curve. In fact, manganin has an optimum operating temperature at which resistivity is maximum and its variation is quadratic.

The available wire shows a quadratic temperature coefficient of -4.5×10^{-7} K^{-2} around the optimum temperature of 20 °C, which is close to the average room temperature.

This optimum temperature has been increased by exploiting the strain gauge effect that arises from the difference between aluminum and manganin linear expansion coefficients (2.3×10^{-5} K^{-1} and 1.8×10^{-5} K^{-1} respectively). The strain gauge effect contributes a temperature coefficient $\delta R/(R\delta T) \simeq 2\delta l/(l\delta T)$, where $\delta l/(l\delta T) \simeq 5\times10^{-6}$ K^{-1} is the expansion coefficient mismatch. Summing this linear effect and the manganin quadratic characteristics results in a parabolic R versus T curve whose maximum is about 10 °C higher than that of manganin. In the described prototype, this optimum working point turns out to be 31.2 °C (Fig. 3), which is sufficiently higher than room temperature to allow easy stabilization. In fact, with a careful design of thermal resistances, the temperature reached by the resistor in the environment by self-heating at the nominal current of 8.6 A can be made close to that optimum. Two Peltier devices stabilize the resistor within 10 mK around 31.2 °C. The main benefit of the above-described design is that the thermal power of the control is minimized, and consequently both the mechanical and electrical effects of temperature gradients inside the resistor are also minimized. In order to minimize thermocouple emfs, power and sensing terminals are also tightly coupled to the thermostat.

Manganin is not easy to solder; moreover, high-temperature heating could alter the crystal lattice and the insulating enamel, thus affecting the resistance stability. For this reason room temperature bonding with Ag-Hg amalgam was used (the well known dentist's amalgam). Before bonding, the surfaces must be carefully cleaned and coated with a thin Hg layer, which amalgamates to the metal below it; this amalgam coating is obtained by dipping the parts — both copper terminals and manganin resistance — in a solution of $HgCl_2$ (5 g/l) and NH_4Cl (25 g/l), as described in [6].

The long-term stability of the amalgam bonding here described has not been investigated because it is beyond our needs. For the same reason, the resistor was not artificially aged in any way.

B. Power Electronics

The power supply was built for this purpose because no commercial equipment readily available fulfilled the ripple specification.

The power supply is energized by three-phase mains, which increases the ripple frequency to 300 Hz after rectification. An LC filter is inserted between the six-phases rectifier and the voltage regulator. The presence of the inductor, which maximizes the conduction angle of the rectifier, prevents high peak currents in the diodes, thus minimizing electromagnetic interference and ground noise. Additional advantages of this configuration are minimum power loss and intrinsic load regulation, limited by parasitic resistances of transformer and inductor.

The series regulator is made using 12 power MOS (IRFP254) connected in parallel. A classic voltage regulator scheme is adopted, with OP27 operational amplifiers, an LT1027 bandgap voltage reference and Vishay-type resistors for best thermal stability. A bandgap reference is preferred to a Zener-based one because of the good noise performances of the former, while the better long-term stability of the latter is not necessary in this part of the circuit; the LT1027 was chosen for its low thermal drift (2×10^{-6}/K).

The power actuator is made using a manganin 0.56 Ω resistor in parallel with a power insulated-gate MOS (IRFP254), and inserted in series between the magnet and the reference resistor. This scheme appeared to be a good choice because i) it has a narrow dynamic range, thus preventing damages in the case of control failure or saturation (this is not irrelevant because of the power involved (800 W) and of the energy stored in the magnet (10 J)); ii) it is safe for human intervention without switching the power off; this last feature is useful because the magnet reaches its thermal steady state a few hours after being powered; and iii) it needs zero driving dc current. This last feature makes it possible to insert the power actuator between load and reference resistor (Fig. 1), thus grounding the latter at one end and consequently minimizing the common-mode voltage at the resistor sensing terminals. The main drawback of this configuration is that the regulator has low transconductance gain: 400 mS in the proposed implementation, which means a 20 dB loss from the MOS driving voltage to the reference resistor output. High-gain amplifiers are needed in the control loop in order to compensate for this loss.

C. Precision Electronic Circuitry

The electronic circuitry must be kept as simple as possible, with a small number of stages, in order to minimize instability sources. A selected version of the OP177 operational amplifier

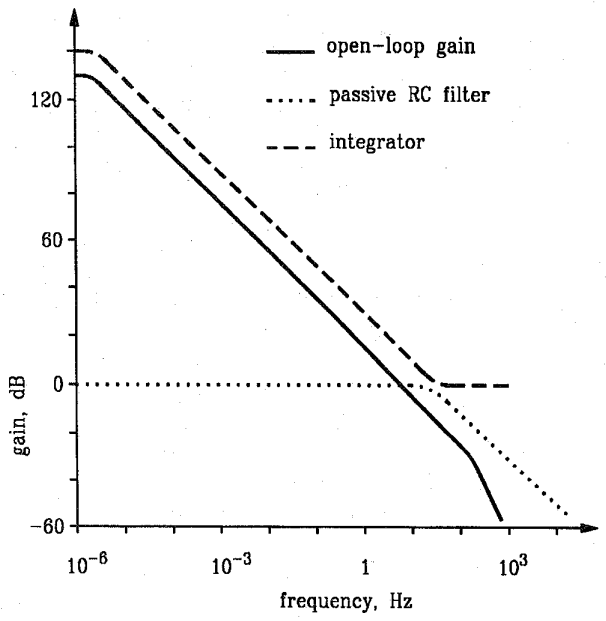

Fig. 4. Bode plots of the current control open-loop gain and its internal stages.

was chosen for all stages, which exhibits open-loop gain and CMRR of 140 dB and thermal drift below 100 nV/K and 100 pA/K in a wide temperature range.

The instrumentation amplifier which senses the voltage across the reference resistor is based on the traditional four-resistor single operational amplifier scheme. The gain is 10 dB, in order to raise the sensed voltage (2.26 V) to 7.15 V, which is the LTZ1000 voltage reference output level. The instrumentation amplifier output is compared to the voltage reference and integrated. A dc bias is added to the integrator output which drives the power actuator; this bias is manually adjusted in order to keep the integrator output around 0 V, thus minimizing leakage currents.

In Fig. 4 Bode plots are shown for the current control open-loop gain and for the most significant internal stages. Since the integrator would have poor high-frequency rejection, limited by the operational amplifier open-loop gain bandwidth product (f_T = 300 kHz), a passive 32 Hz low-pass network (dotted line) is inserted in the loop. In order to compensate the passive low-pass filter phase lag, which is necessary to prevent servo loop instability, the integrator transfer function (dashed line) has a zero at 32 Hz. The solid line with slope -1, crossing 0 dB at 7 Hz, is the open-loop gain of the whole control, which includes other stages whose transfer function is not shown in the figure. The dc gain (about 130 dB) is not easy to identify exactly because it includes the open-loop gain of the integrator operational amplifier.

All resistors in the instrumentation and summing amplifiers, and in the voltage reference, are of the Vishay type.

The electronic circuits are enclosed in a box made of 15 mm and 25 mm thick aluminum plates, Silicone™ sealed and filled with anhydrous nitrogen. This box is thermally stabilized within 50 mK around the average room temperature. In order to keep as stable as possible the temperature of the most critical resistors — the Vishay ones responsible for the instrumentation and summing amplifier gains — these resistors are mounted inside a copper block tightly coupled to the aluminum box. The NTC resistor responsible for temperature stabilization of the box is also placed inside the same copper block.

III. Stability Analysis

The field measurement problem involves the concept of stability as a function of averaging time, i.e., a measurement time between a few seconds (spot measurement) and 1–2 h, which is the maximum duration of the probe travel along the magnet. In the presence of some types of noise (such as flicker and random walk) the standard deviation — as usually defined in statistics — depends on the number of measurements, diverging as the sample size increases. The Allan deviation $\sigma(\tau)$, proposed in [7] for use in the field of atomic clocks, is a suitable mathematical tool not affected by the divergence problem. Consequently, it was decided to express the stability in terms of Allan deviation.

The most relevant instability causes in the proposed circuit are summarized in Table I which reports, for each parameter, the minimum specification for a contribution not greater than 10^{-7} to the overall instability.

The LTZ1000 voltage reference shows a temperature coefficient of 2×10^{-8}/K and a long-term stability below 10^{-6} (one year) in a proper circuit [8]. As a consequence, it can be considered ideally stable in this application.

The analysis of stability problems in the electronic circuitry shows some unusual aspects. These are discussed below.

1) Resistance values should be chosen in the 1 kΩ to 10 kΩ range for best stability. When using smaller values, cables and printed circuit boards must also be included in the model. For example, a typical copper printed circuit strip 1.25 mm wide, 25 mm long, 35 μm thick, has a resistance of 10 mΩ with a thermal coefficient of 3.4×10^{-3}/K; an ideal 100 Ω resistor connected in series to this parasitic resistance acquires a bias error of 10^{-4} and a thermal coefficient of 3.4×10^{-7}/K. Moreover, it is a safe rule to avoid load resistances smaller than about 1 kΩ at the output of operational amplifiers, in order to prevent self-heating of the output stage. In fact, the typical thermal resistance Θ_{jA} (junction-air) of an eight-pin plastic dual-in-line package is not less than 100 K/W. Resistance values higher than tens of kilohms make the circuit sensitive to leakage currents, and consequently to humidity fluctuations.
2) The gain of the instrumentation amplifier must have a stability of 10^{-7}. The summing amplifier output is the error signal $V_e = A_x V_x + A_r V_r$, where V_r is the reference voltage, V_x is proportional to current, and A_r and A_x are the amplifier gains. The gain ratio A_x/A_r must have a stability of 10^{-7}.
3) The resistance ratios responsible for the gain of instrumentation and summing amplifiers must have at least a stability of 10^{-7}. This is a very severe requirement. Some attempts were made to build high-

TABLE I
STABILITY BUDGET. FOR EACH PARAMETER, THE MINIMUM SPECIFICATION IS REPORTED FOR A CONTRIBUTION NOT GREATER THAN 10^{-7}

Parameter	Limit	Conditions or comments
reference resistor stability	$\frac{\delta R}{R} < 10^{-7}$	
thermal emfs	$\delta V < 230$ nV	1) voltage across the ref. resistor is 230 mV 2) nonclimatized laboratory conditions
voltage reference stability	$\frac{\delta V}{V} < 10^{-7}$	
I.A. gain stability	$\frac{\delta A}{A} < 10^{-7}$	
I.A. operational amplifier open loop gain	$A_{\mathrm{dB}} > 130$ dB	I.A. operational amplifier open-loop gain stability 10% or better
I.A. drift	$\delta V < 230$ nV	voltage across the ref. resistor is 230 mV
I.A. CMRR	$\mathrm{CMRR}_{\mathrm{dB}} > 93$ dB	10 mV max. voltage drop across cables
summing amplifier gains ratio stability	$\frac{\delta A_x/A_x}{\delta A_r/A_r} < 10^{-7}$	
summing amplifier drift	$\delta V < 700$ nV	I.A. gain 10 dB
stability of critical resistance ratios	$\frac{\delta R_1/R_1}{\delta R_2/R_2} < 10^{-7}$	this limit is included in the specifications of the instrumentation and summing amplifiers
integrator dc gain	$A_{\mathrm{dB}} > 127$ dB	needed for a total loop gain of 120 dB

stability matched resistor pairs using 40 μm diameter manganin wire, with a resistance per unit length of 325 Ω/m. Unfortunately, it was not possible to take full benefit of the manganin parabolic resistivity versus temperature curve because hand-wound resistors ended up having a scarcely reproducible average strain in the wire, which shifted the temperature of the resistance maxima by unpredictable amounts. The best thermal coefficient that could be obtained for the ratio was of the order of 10^{-6}/K. On the other hand, the best commercially available (Vishay) resistors also have a thermal coefficient not smaller than 10^{-6}/K (besides a small thermal hysteresis which is not a problem in this application). Thermal coupling of two of these resistors does not improve the stability of their ratio because the residual thermal sensitivity of each resistor results from imperfect compensation between two physical effects with opposite sign. Resistance ratios of Vishay-matched pairs are more stable by a factor of about two, which is not sufficient. After a few attempts, it became clear that attaining the stability of 10^{-7} without temperature stabilization was not possible either with in-house fabricated manganin pairs or with Vishay resistors.

4) The open-loop gain of operational amplifiers must also be considered carefully for the 10^{-7} stability goal. Let us analyze a stage whose gain is a critical parameter, either the instrumentation or the summing amplifier. While the nominal gain $G_n = 1/\beta$ of the amplifier is determined by the feedback network gain β, the actual gain G has a bias error $(G - G_n)/G = \Delta G/G = -1/(A\beta)$, where A is the operational amplifier open-loop gain. The consequence of an open-loop gain instability $\delta A/A$ is an instability $\delta G/G = (1/A\beta)(\delta A/A)$. The open-loop gain A is affected by temperature and supply voltage; practical values are $\delta A/(A\delta T) \simeq 6\times10^{-3}/\mathrm{K}^{-1}$, and $\delta A/(A\delta V) \simeq 5\times10^{-2}/\mathrm{V}^{-1}$ for a selected OP177. The most relevant effect seems to be the crossover distortion, by which the open-loop gain decreases in the vicinity of 0 V output: the consequence of this is a gain instability related to the DC bias. The effect of crossover distortion on the open-loop gain is discussed in [9]. In analyzing data sheets of operational amplifiers, one should note that gain linearity is not specified in quantitative terms, although this problem is sometimes mentioned. For high-quality devices, the assumption $\delta A/A \leq 10^{-1}$ seems to be conservative. The practical implication of this is that, assuming for instance $\beta = 0.3$ ($G \approx 10$ dB) and $\delta A/A = 10^{-1}$, a minimum open-loop gain $A = 3\times10^6$ (130 dB) is needed for a gain stability of 10^{-7}.

5) The common-mode rejection ratio is not a serious problem in this application. This happens because most of the common-mode signal is half of the voltage across the reference resistor, which is stabilized. The only contribution to common-mode voltage change is originated by the voltage drop on cables (less than 100 mV), which has a thermal coefficient of 3×10^{-3}/K (due to copper

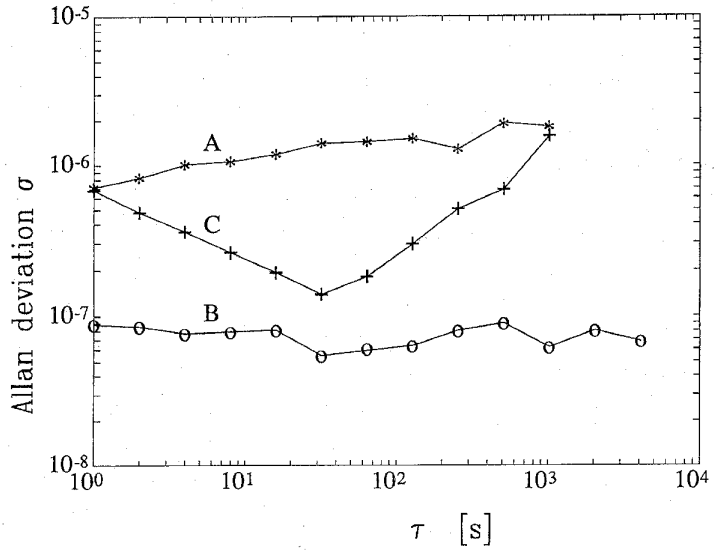

Fig. 5. Experimental results of stability measurements.

resistivity) and random variations well below 1 mV. After a careful matching of the instrumentation amplifier resistances, a CMRR in excess of 110 dB was obtained, which guarantees that the common-mode variations have a negligible effect.

6) The temperature of the electronic circuits is a critical point because it affects resistance ratios and operational amplifier offsets; high-performance operational amplifiers have low thermal drift, in some cases below 100 nV/K without chopper stabilization. Temperature gradients, which can arise in the presence of temperature fluctuations, must be considered carefully because in the electronic circuitry there are many contacts between different materials. For example, the Seebeck coefficient between the Kovar pins of integrated circuits and the copper of leads or printed circuit metallization is about 30 μV/K [10]. Consequently, a temperature difference of a few millikelvin between two "bad" points of the circuit can change the magnet current by 10^{-7}. The obvious cure would be an oil bath, which should keep the whole circuit at the same temperature. Unfortunately, unless a cumbersome mechanical design is chosen, this solution does not fit the proposed circuit because the LTZ1000 internal thermostat needs a high thermal resistance between case and environment for proper operation.
7) The effect of environmental humidity variation has been minimized by filling the electronic circuit box with anhydrous nitrogen. The benefit of this technique is obvious, but was not analyzed quantitatively.

The long-term instability of active devices has been analyzed by translating worst case specifications into voltage Allan deviation. It should be observed that, while flicker and white noise coefficients can be easily drawn from data sheets, the long-term behavior is usually specified as the voltage variation after one month, which is ambiguous. In fact, this parameter includes the contribution of both random walk and linear drift. When trying to translate this specification into Allan deviation, one should note that these processes are represented by stright lines with different slope (1/2 and 1 respectively) in the log-log σ-τ plane, while only the total value for $\tau = 2.6\times10^6$ s (one month) is specified. In order to give conservative estimates, the specification has been interpreted as a pure random walk process, which gives the worse stability in the short-medium term, where $\tau \ll 2.6\times10^6$ s. Surprisingly, none of these noise processes, flicker, white and "random walk," is a serious problem in the present application.

IV. Measurements and Results

The stability of the 0.26 Ω reference resistor, operating at its nominal current, has been measured by comparing the resistor to a 0.1 Ω standard in a Kelvin bridge. The temperature of this standard has been stabilized by an adequate thermal capacitance (4 kg Vaseline oil) and monitored in order to remove its effect from the results. All of the low-current resistors of the bridge were of the Vishay type, thermally stabilized within 10 mK. The resistance stability turned out to be 1.2×10^{-7} over many hours, which is satisfactory. This value is only an upper bound for the reference-resistor instability because it includes zero-detector noise and power-supply instability, and is affected by residual thermal effects, mainly due to the uncertainty of the standard's temperature coefficient.

The circuit described in this paper was used to stabilize the current supplied to the magnet.

The statistical deviation of the error signal, inside the control loop, is equivalent to a current deviation in the 10^{-8} range. This value indicates that the electronic circuitry works properly, but cannot be taken as a measure of current stability because it does not include the instability of reference resistor and instrumentation amplifier gain. The current stability must

be determined by measuring the voltage drop across the reference resistor.

Stability results, described in terms of Allan deviation $\sigma(\tau)$, are shown in Fig. 5. When the current control is not in operation, the current stability is limited by the power supply. This is shown by curve A, which represents the Allan deviation of the voltage sensed at the reference resistor terminals in open-loop conditions. Curve B is the Allan deviation of the voltage (proportional to current) measured across the reference resistor in normal control operation. The stability is about 8×10^{-8}, which is satisfactory. The actual current stability may be slightly worse than shown because this measurement does not include the reference resistor instability. The average slope of curve B is about zero, which reveals that the stability is limited by flicker noise.

The Allan deviation $\sigma(\tau)$ averaging mechanism acts as a bandpass filter whose center frequency is $f \simeq 1/2\tau$. When translating the control open-loop gain (Fig. 4) from a function of frequency into a function of τ in order to compare it to the plot of Fig. 5, the gain is represented by a straight line whose slope is $+1$, crossing the 0 dB axis at $\tau = 70$ ms. The difference between curves A (power supply stability) and B (current stability) of Fig. 5 turns out to be smaller than the open-loop gain for all τ values of that figure. This shows that the current stability is limited by instabilities within the control itself, and hence that the loop gain is adequate for the application.

Curve C is the Allan deviation of the magnetic field, measured with an NMR probe in the center of the magnet.

In the left part of the figure, curve C is limited by a white noise process $\delta B/B \simeq 7\times10^{-6}\tau^{-1/2}$, which crosses the flicker floor at $\tau \approx 100$ s. This process is originated by poor S/N ratio in the NMR probe. In fact, it is absent in the current, and there is no reason to believe that it is generated by the magnet.

In the right part of curve C ($\tau > 30$ s) a drift process (slope +1) is evident, which is thought to be originated by changes in the I to B conversion. Under the assumption of infinite μ_r magnetic return path, the expected effect of a thermal dilation $\delta l/l$ is a change $\delta B/B \simeq -\delta l/l$ in the magnetic field. The measured thermal effect turns out to be about 4 times higher than that. The reason for this difference is not yet understood for the available magnet and needs investigation, but this is beyond the purpose of this paper. However, it should be pointed out that, taking into account the thermal expansion coefficient of copper (1.7×10^{-5} K^{-1}), a temperature fluctuation of the order of 15 mK will originate a 10^{-6} field instability.

V. Conclusion

A control circuit has been described, that stabilizes 10 A dc currents for energizing magnets. The proposed design criteria have allowed the realization of a prototype whose stability is about 10^{-7} from a few seconds to 1 or 2 h, without using chopper amplifiers. The field stability is presently limited by geometric factors in the magnet.

Acknowledgment

The author would like to thank G. Costanzo, who performed most of the stability measurements, A. De Marchi, for many scientific discussions and a careful revision of this work, and E. Angelini, for her suggestions on chemistry.

References

[1] A. De Marchi, "The high C-field concept for an accurate cesium beam resonator," in *Proc. 6th Euro. Frequency and Time Forum,* Neuchâtel, Switzerland, March 1993, pp. 541–548.
[2] A. De Marchi, G. Costanzo, C. Lombardi, A. Del Casale, F. Maddaleno, E. Rubiola, M. Repetto, and M. Chiampi, "A high uniformity magnet for a high C-field cesium beam resonator," in *Proc. 6th Euro. Frequency and Time Forum,* Neuchâtel, Switzerland, March 1993, pp. 367–371.
[3] G. Costanzo, A. De Marchi, M. Nervi, and M. Repetto, "High homogeneity solenoidal magnet for cesium frequency standard," *IEEE Trans. Magn.,* vol. 30, no. 4, pp. 2628–2631, July 1994.
[4] G. Costanzo, M. Nervi, M. Repetto, and F. Levati, "Use of automated optimization techniques in the design of the magnetic system for a cesium frequency standard," in *3rd Workshop Optimization and Inverse Problems in Electromagnetism,* CERN, Geneve, Switzerland, Sept. 19–21, 1994. To be printed in *Int. J. Appl. Electromagn. Mater.*
[5] G. Costanzo, "Ottimizzazione di un campione atomico di frequenza a fascio di cesio," Ph.D. dissertation, Politecnico di Torino, 1995.
[6] E. Bertorelle, *Trattato di Galvanotecnica.* Milano, Italy: Ulrico Hoepli, 1974.
[7] D. W. Allan, "Statistics of atomic frequency standards," *Proc. IEEE,* vol. 54, p. 221–230, Feb. 1960.
[8] P. J. Spreadbury, "The ultra zener: A portable replacement for the Weston cell?," *IEEE Trans. Instrum. Meas.,* vol. 40, p. 343–346, April 1991.
[9] D. L. Feucht, *Handbook of Analog Circuit Design.* New York: Academic, 1990.
[10] S. Soclof, *Analog Integrated Circuits.* New York: Prentice-Hall, 1990.

Enrico Rubiola was born in Torino, Italy, in 1957. He received the degree in electronic engineering and the Ph.D. degree from the Politecnico di Torino, Italy, in 1983 and 1989, respectively.

He is currently a Researcher at the Politecnico di Torino. His main areas of interest are time and frequency metrology, methods of comparison and dissemination, frequency synthesis, and precision electronics.